Since January 2020 Elsevier has created a COVID-19 resource centre with free information in English and Mandarin on the novel coronavirus COVID-19. The COVID-19 resource centre is hosted on Elsevier Connect, the company's public news and information website.

Microchemical Journal 184 (2023) 108195

Contents lists available at ScienceDirect

Microchemical Journal

journal homepage: www.elsevier.com/locate/microc

Voltammetric determination of Molnupiravir used in treatment of the COVID-19 at magnetite nanoparticle modified carbon paste electrode

Kader Vural [a], Serkan Karakaya [b,*], Didem Giray Dilgin [a], Hatice İsmet Gökçel [c], Yusuf Dilgin [b,*]

[a] Çanakkale Onsekiz Mart University, Faculty of Education, Secondary Science and Mathematics Education Department, 17100 Çanakkale, Turkey
[b] Çanakkale Onsekiz Mart University, Faculty of Science, Chemistry Department, 17100 Çanakkale, Turkey
[c] Ege University, Faculty of Science, Department of Chemistry, 35100 Bornova-İzmir, Turkey

ARTICLE INFO

Keywords:
Molnupiravir
COVID-19
Magnetic Fe_3O_4 nanoparticles
Carbon paste electrode
Cyclic voltammetry
Electrochemical sensor

ABSTRACT

To reduce the progression of the viral process in patients infected with COVID-19, new treatments and drug active substances are needed. One of these drugs is Molnupiravir (MNP) which has a direct antiviral effect and has also proven to be highly effective in reducing the azopharyngeal SARS-CoV-2 infectious virus and viral RNA. Due to the importance and frequent use of this drug in the treatment of COVID-19, its accurate, quick, and cheap detection in pharmaceutical or biological samples is crucial. In this work, electrochemical behavior and sensitive voltammetric determination of MNP are described using a magnetite nanoparticle modified carbon paste electrode (Fe_3O_4@CPE) for the first time. Fe_3O_4 nanoparticles (NPs) were characterized by recording their transmission electron microscopy (TEM) images, energy dispersive X-ray (EDX), and X-ray diffraction (XRD) spectra. Cyclic voltammetric measurements showed that MNP was irreversibly oxidized at Fe_3O_4@CPE at 760 mV in pH 2.0 Britton Robinson buffer solution (BRBS). The peak current of MNP was increased approximately threefold at Fe_3O_4@CPE compared to bare CPE due to a good electrocatalytic efficiency of Fe_3O_4 NPs. According to differential pulse voltammetric studies, the fabricated electrode exhibited a linear range (LR) between 0.25 and 750 μM with sensitivity and limit of detection (LOD) of 4591.0 μA mM^{-1} cm^{-2} and 0.05 μM, respectively. On the other hand, although lower sensitivity (327.3 μA mM^{-1} cm^{-2}) was obtained from CV compared to DPV, a wider linear calibration curve between 0.25 and 1500 μM was obtained in CV. Studies performed in tablet samples confirmed that the Fe_3O_4@CPE exhibits high applicability for selective and accurate voltammetric determination of MNP in real samples.

1. Introduction

The new type of coronavirus (COVID-19, also known as SARS-CoV-2) was first detected in December 2019, in Wuhan, China, and has an ongoing impact all around the globe, especially because of the recently emerged variants such as Delta, Omicron, and Ba.2. On 11th March 2020, the World Health Organization (WHO) declared the COVID-19 outbreak to be a global pandemic [1]. More than 630 million cases and more than 6.5 million deaths were reported by WHO on 9th November 2022 [2]. While vaccine studies are being conducted to combat COVID-19, several existing antiviral drugs that have previously proven effective and safe against other viruses have been urgently used for the treatment of COVID-19.

One of these drugs is Molnupiravir (MNP) known as *N*-Hydroxy-5′-O-isobutyryl-3,4-dihydrocytidine [(2R,3S,4R,5R)-3,4-Dihydroxy-5-[4-(hydroxyamino)-2-oxopyrimidin-1-yl]oxolan-2-l]methyl 2-methylpropanoate with commercial cod (EIDD-2801 and MK-4482) (Scheme 1 in the oxidation mechanism of MNP) [3]. It was originally developed by the university's drug innovation company (Drug Innovation Ventures at Emory (DRIVE)) at Emory University for the treatment of influenza [4]. Several synthesis routes, along with the synthetic route proposed by Emory University in 2019 to obtain MNP, are given in a review article [5]. To develop this drug, Merck & Co and Ridgeback Biotherapeutics companies made a partnership and a new oral anti-viral drug was launched [6,7]. Owing to favorable results obtained from placebo-controlled double-blind randomized clinical trials; MNP was affirmed for medical treatment in the UK in November 2021 [8]. In December 2021, the U.S. Food and Drug Administration (FDA) granted emergency use authorization of MNP for use in certain populations where other treatments are not available [9]. MNP, an oral ribonucleoside analog

* Corresponding authors.
E-mail addresses: 23karakayaserkan@gmail.com (S. Karakaya), ydilgin@yahoo.com (Y. Dilgin).

https://doi.org/10.1016/j.microc.2022.108195
Received 16 July 2022; Received in revised form 14 November 2022; Accepted 15 November 2022
Available online 17 November 2022

with broad-spectrum antiviral activity, is a prodrug of the synthetic nucleoside derivative N4-hydroxycytidine (NHC) and exerts its antiviral effect through the insertion of transcription errors during viral RNA replication. MNP blocks the replication of SARS-CoV-2 in the lines of cells, culture media containing respiratory epithelial cells, and animal-infected models and has been suggested as a potential therapy for COVID-19 [3]. In conclusion, MNP has broad antiviral activity against RNA viruses, and the uptake of NHC by viral RNA-dependent RNA polymerase (RdRp) causes viral mutations and lethal mutagenesis. In this way, MNP shows potent antiviral activity against SARS-CoV-2.

The development of sensitive, accurate, low-cost, reliable analytical methods is required for the monitoring and determination of this important drug in different matrices such as biological fluids and pharmaceutical preparations. The determination of this newly developed drug in both pharmaceutical samples and body fluids is very important, and thus studies on detection methods have recently been started. In the first studies, various chromatographic methods have been developed for the determination of MNP such as reversed phase-high performance liquid chromatography (RP-HPLC) with a photodiode array detector (UV measurement at 240 nm) [10], HPLC with UV detector [11] and LC-MS/MS [12]. Although chromatographic methods offer selective and simultaneous determination of MNP with together other drugs or its metabolites, these methods need some requirements such as time-consuming sample preparation steps, highly trained personnel, highly cost instrumentation, high solvent consumption, and complicated procedures. Therefore, the development of simple, selective, and sensitive new alternative methods in drug analysis has always been of interest.

Among the various analytical methods, electroanalytical methods have been widely used for the determination of various compounds in pharmaceutical samples because they offer great advantages such as high simplicity, easy operation, portability, low cost, miniaturization, rapid response, acceptable sensitivity, accuracy, precision, and selectivity [13–18]. In electrochemical measurements, both bare and modified electrodes have been extensively used in pharmaceutical analysis. However, bare electrodes show poor sensitivity and selectivity due to high background current and overpotentials, heterogeneous and passive surface, and slow redox kinetics in electrochemical reactions of many compounds. These limitations have been overcome by modifying the electrode surfaces with new synthetic materials and modifiers [19]. In this direction, many researchers have recently reconstructed the electrode surfaces by modifying them with nanomaterials to improve the sensitivity and selectivity and to provide excellent electrocatalytic potentials owing to their beneficial properties such as large active surface area, good electrical conductivity, high surface/volume ratio [19–22]. Carbon paste electrodes (CPEs) are one of the most commonly used electrodes in the fabrication of modified electrodes because they offer some advantages such as ease of fabrication and modification, renewable surface, low residual current, low cost, porous structure, chemical inertness, good reproducibility, and stability [23,24]. Due to their important properties such as a high ratio of surface area to volume, strong adsorption ability, and electrocatalytic activity, metal or metal oxide nanomaterials have been frequently preferred in the preparation of CPE-modified electrodes [23–28]. Metal oxides are active and durable electrocatalysts for the construction of sensors and biosensors [29]. Among the nanomaterials, magnetite nanoparticles (Fe_3O_4 NPs) have attracted growing interest in recent years in electroanalysis because they have advantages over other oxides in terms of their high theoretical capacity of 922 mAh g^{-1}, eco-friendliness, natural abundance, low particle size, low-cost production, controllable and large active surface area, ease of preparation, strong superparamagnetic, nonpoisonous, electrical conductivity, biocompatibility, and catalytic properties [29–31]. Therefore, Fe_3O_4 NPs have been widely used as modification material for electrode surfaces in fabricating sensors/biosensors [19,23–37]. In particular, the modification of CPE with Fe_3O_4 NPs, which involves a very simple preparation procedure, yields an efficient surface area and good electrocatalytic activity on the bare electrode surface. Thus, an efficient mass transfer is achieved by mediating electron transfer between the electroactive species and the electrode surface by using a graphite/Fe_3O_4 system, as well as an easily prepared modified CPE with a low-cost and renewable surface is obtained [23].

According to our literature search, the first electrochemical study on MNP determination using a reduced graphene oxide modified glassy carbon electrode (rGO/GCE) was reported by Nemutlu et al [38]. Although rGO/GCE [38] offers high sensitivity, reproducibility, and stability for MNP analysis, a time-consuming modification procedure was used with expensive electrode materials. In addition, a theoretical electrochemical study has been reported for MNP and the possibility of electrochemical determination of MNP was evaluated as theoretical [39]. Electrochemical oxidation of MNP on a composite material containing poly((1,2,4-triazole)-co-(squaraine dye)) and cobalt(III) oxyhydroxide was theoretically examined in this published study. In our study, Fe_3O_4@CPE used provides an easily prepared renewable electrode surface and includes a simple and low-cost modification procedure. Moreover, the electrode used has a competitive detection limit compared to the rGO/GCE [38]. Thus, the novelty of this study is the development of a sensitive, selective, and stable electrochemical method for MNP analysis with a simple, easily prepared, low-cost electrode (Fe_3O_4@GCE) whose electrode surface can be easily regenerated. The feasibility of the fabricated electrode was investigated by performing the determination of MNP in a pharmaceutical sample and recovery studies in pharmaceutical samples spiked with MNP. The fabricated electrode exhibits highly sensitive, selective, repeatable, and reproducible results with high recovery values for the determination of MNP in real samples.

2. Materials and methods

2.1. Chemicals and instrumentation

Molnupiravir ($C_{13}H_{19}N_3O_7$, 98 %, 329.31 g/mol) and graphite (fine powder extra pure, particle size $\leq$ 50 μm, and bulk density 20–30 g/100 mL) were supplied from Merck. Mineral oil with spectroscopic grade was supplied from Sigma-Aldrich. All other chemicals used in this study are of analytical grade.

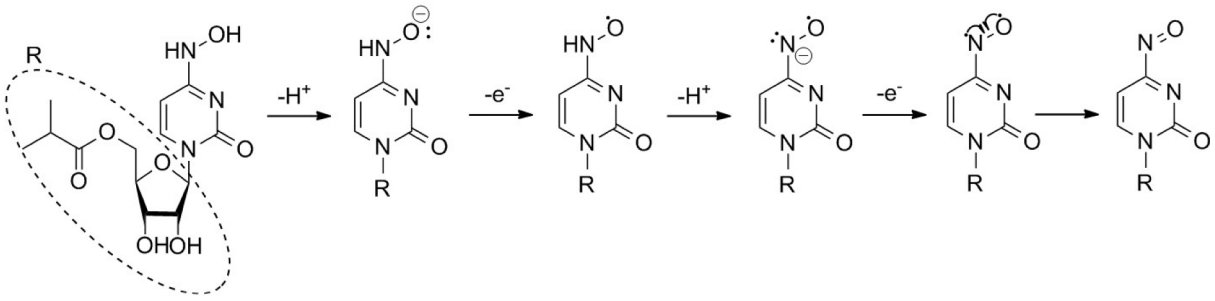

Scheme 1. A possible mechanism for the electrocatalytic oxidation of MNP.

All electrochemical experiments were performed by using an interface compactstat device with Ivium technologies (from Netherlands) and an electrochemical cell with a classical three-electrode system: (i) working electrode: BASI carbon paste electrode (Geometric area (GA): 0.065 cm^2 diameter: 2.87 mm), (ii) reference electrode: BASI-RE5B $Ag/AgCl_{(sat.\ KCl)}$ (diameter: 6.0 mm, length: 7.5 cm) and (iii) counter electrode: BASI-MW1032 Pt wire (diameter: 0.5 mm, length: 7.5 cm). An Elga Option-Q7B device was utilized to get ultra-pure water (18.2 MΩ cm^{-1}) for the preparation of all solutions. The pH values of buffer solutions were measured with a Hanna HI-221 pH-meter with a combined glass electrode. TEM micrograph, EDX, and XRD spectra of Fe_3O_4 NPs were recorded using a JEOL JEM-1400 PLUS, JEOL SEM-7100-EDX, and XRD PANalytical Empyrean devices in the Applying Science and Technology Center of Çanakkale Onsekiz Mart University (ÇOBİLTUM). A stock MNP solution (0.01 M) was prepared by dissolving 0.033 g of MNP in 10 mL of methanol. Britton Robinson buffer solutions (BRBSs) were prepared in the pH range between 2.0 and 10.0 from 0.10 M KCl solution containing 0.04 M CH_3COOH, 0.04 M H_3BO_3, and 0.04 M H_3PO_4. The pH value of BRBS was adjusted by the addition of 0.20 M NaOH solution containing 0.10 M KCl.

2.2. Preparation of Fe_3O_4@CPE

The magnetic Fe_3O_4 NPs were prepared according to a reported procedure [40]. To prepare the Fe_3O_4 modified carbon paste electrode, the graphite powder, Fe_3O_4 NPs, and mineral oil were mixed with a ratio of 65:5:30 (w/w %), respectively, and the electrode body was filled with this prepared paste. The surface of the modified CPE was polished on the coated paper and the resulting electrode was named Fe_3O_4@CPE.

2.3. Electrochemical studies

To investigate electrochemical characterizations of the electrodes before the electrochemical study of MNP, cyclic voltammograms (CVs) and electrochemical impedance spectra (EIS, in the frequency range from 0.10 to 100000 Hz) of both bare and modified CPEs were recorded in the redox probe of 5.0 mM $Fe(CN)_6^{4-/3-}$ in 0.10 M KCl.

Cyclic voltammetry was used to investigate the electrochemical behavior of MNP. In this context, CVs of 0.10 mM MNP were recorded in the potential scan range from 0.30 to +1.0 V in the BRBS containing 0.10 M KCl with varied pH in the range from 2.0 to 7.0 at a scan rate of 50 mV s^{-1}. CVs of 0.10 mM MNP were also recorded dependent on scan rate varied between 10 and 1200 mV s^{-1} in pH 2.0 BRBS containing 0.10 M KCl. In the final step, CVs of MNP were recorded based on the increasing concentration of MNP in the range from 0.25 to 1500 μM in pH 2.0 BRBS containing 0.10 M KCl. In addition, analytical performance studies of MNP were also performed by recording differential pulse voltammograms (DPVs) of MNP. In all experiments, highly pure Ar was purged from supporting electrolytes for 5 min.

2.4. Real sample studies

A pharmaceutical tablet was used to see the feasibility of the fabricated electrochemical method. The pharmaceutical tablet with a labeled 200 mg MNP per tablet was supplied from a pharmacy in İzmir, Turkey.

In the pharmaceutical analysis, five pharmaceutical tablets were weighed and grounded in agate mortar until fine homogenous powders were obtained. An amount of homogenized powders equal to one tablet weight was weighed and then dissolved in 25 mL methanol. After approximately 10 min of sonication, an aliquot volume of this sample was diluted in a volumetric flask of 10 mL with methanol to obtain an appropriate pharmaceutical solution including about 500 μM MNP. Then a known volume of diluted pharmaceutical solution was transferred to the supporting electrolyte of pH 2.0 BRBS containing 0.10 M KCl, and DPVs were recorded based on the standard addition method. In addition, a pharmaceutical solution including about 50 μM MNP was spiked as 25.0, 50.0, and 100.0 μM MNP, and recovery studies were performed for each spiked sample by recording standard addition DPVs.

3. The results and discussions

3.1. Optimization of the amount of Fe_3O_4 in modified CPE

To see the effect of the amount of Fe_3O_4 in the modified CPE on the voltammetric response of the MNP, modified carbon paste electrodes containing different ratios of Fe_3O_4 in the range from 0.0 to 10.0 % were prepared. Then CVs of each modified electrode were recorded in pH 2.0 BRBS containing 0.10 M KCl in the presence of 0.5 mM MNP at a scan rate of 50 mV s^{-1}. According to the recorded voltammograms (Fig. S1A) and the curve of peak current versus %Fe_3O_4 in the modified CPE (Fig. S1B), the oxidation current of MNP increased proportionally with increasing Fe_3O_4 amount from 0.0 % to 5.0 % and did not change much after 5.0 % Fe_3O_4. Thus, a 5.0 % Fe_3O_4 amount in the modified electrode was determined as the optimum value, and modified CPEs prepared at this ratio were used in all following studies.

3.2. Characterization of the Fe_3O_4@CPE

Electrochemical impedance spectroscopy (EIS) gives valuable information about the surface conductivity of the modified electrode surface. Thus, EI spectra of both bare and modified electrodes were recorded in the solution of 0.10 M KCl + 5.0 mM $Fe(CN)_6^{3-/4}$ (Fig. S2A). It is seen from the Nyquist diagram of bare CPE (Fig. S2A-a) that it has a very high charge transfer resistance (R_{ct} = 1330 Ω), while this R_{ct} value is considerably reduced by modifying of the CPE surface with Fe_3O_4 NPs (R_{ct} = 853 Ω, Fig. S2A-b). The decrease in R_{ct} value is attributed to the increase in the effective surface area of the electrode, and the electroactive sites due to the good conductive properties of Fe_3O_4 NPs. Therefore, it was concluded that the Fe_3O_4 NPs improved the surface conductivity properties of the CPE. Fig. S2B shows the CVs of the bare and modified electrodes in the same redox probe solution. Compared to bare CPE (Fig. S2B-a), the increases observed in the peak currents of the redox couple of ferro/ferri cyanides at Fe_3O_4@CPE support the results of the EIS analysis.

The morphological characterization studies were carried out by recording the TEM micrographs, EDX, and XRD spectra of Fe_3O_4 NPs. As can be seen from the TEM micrographs, the dispersion of the Fe_3O_4 NPs is nearly spherical and the size of the nanoparticles differs between 12 and 18 nm (Fig. 1A). The recorded EDX spectrum also reflects the elemental components (33.7 % Fe and 66.1 % O) of Fe_3O_4 NPs (Fig. 1B). The crystal structure of Fe_3O_4 NPs was examined by XRD and the diffraction patterns of Fe_3O_4 are given in Fig. 1C. As can be seen from the figure, the characteristic peaks observed at 2Θ degree of 30.45, 35.77, 43.41, 53.69, 57.52 and 63.16 are attributed to the (2 2 0), (3 1 1), (4 0 0), (4 2 2), (5 1 1) and (4 4 0) crystal planes of Fe_3O_4 NPs which are in good agreement with standards (JCPDS19-0629) and the Fe_3O_4 NPs show spinel structure of cubic inverse [40]. All results obtained from TEM, EDX, and XRD analyses support the successful synthesis of magnetite nanoparticles.

3.3. Determination of the electroactive surface area

The electroactive surface area of the bare CPE and Fe_3O_4@CPE was further examined by evaluating the current response of $Fe(CN)_6^{3-/4-}$ redox probe from Fig. S2B. As can be seen from the Fig. S2B, Fe_3O_4@CPE displays an improvement in the current response, in other words, the electrochemically active sites of bare CPE were increased by the modification of the Fe_3O_4 NPs onto the surface. As a result, the Fe_3O_4@CPE gives a higher current response (I_{pa} = 33.1 μA) compared with the bare CPE (I_{pa} = 12.7 μA) due to the electrocatalytic activity of the Fe_3O_4 NPs. The electroactive surface area of the electrodes was estimated according to the Randles–Sevcik Eq. (1) [23,38,41].

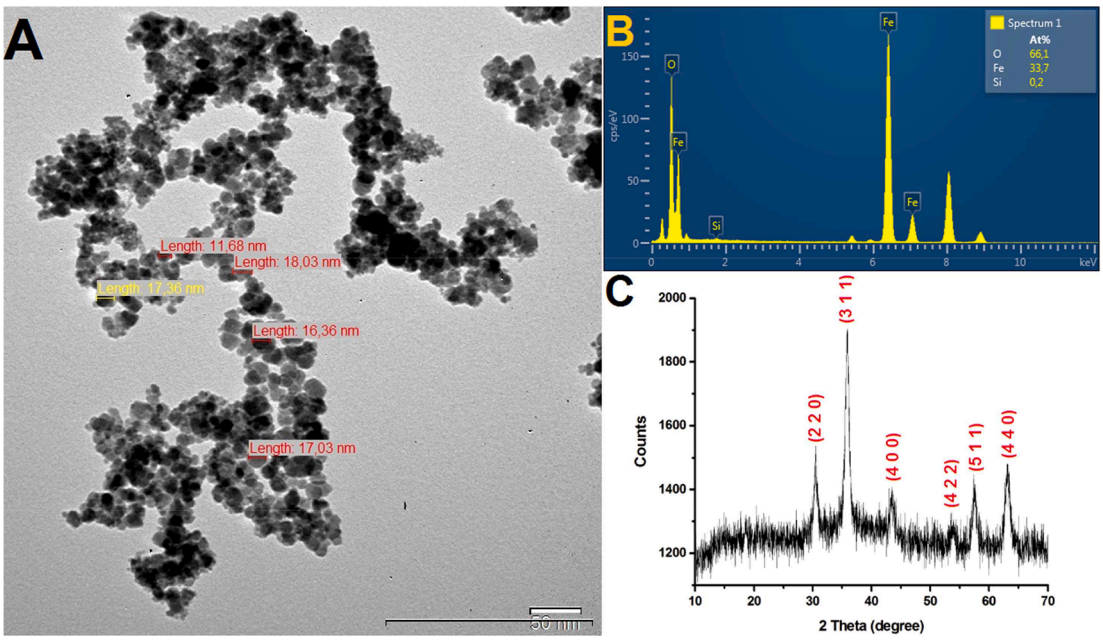

Fig. 1. TEM micrograph **(A)**, EDX spectrum **(B)**, and XRD patterns **(C)** of the synthesized Fe_3O_4 NPs.

$$I_{pa} = 2.69 \times 10^5 n^{3/2} A C_o D^{1/2} v^{1/2} \quad (1)$$

"I_{pa}" is oxidation current (A), "n" is the electron number (which is equal to one), "A" is the area of the active surface (cm^2), "C_o" is the concentration of the $Fe(CN)_6^{3-/4-}$ (5.0×10^{-6} mol cm^{-3}), "D": diffusion coefficient of $Fe(CN)_6^{4-}$ (6.23×10^{-6} cm^2 s^{-1}) [23]. The electrochemically active surface areas were calculated as 0.044 cm^2 and 0.017 cm^2 for Fe_3O_4@CPE and CPE, respectively. In the literature, very close specific surface area values have been obtained in Fe_3O_4/CPEs prepared for use in the determination of various phenolic compounds [23] and simultaneous determination of ascorbic acid and folic acid [28]. The results indicate that the modification of Fe_3O_4 NPs enhanced (~3 times) the electrochemically active area of the electrode surface.

3.4. Electrochemical behavior of MNP at Fe_3O_4@CPE

The electrochemical response of both bare and modified CPEs in a pH 2.0 BRBS containing 0.10 M KCl towards 0.10 mM MNP was further investigated for the suitability of the respective modified electrode for the determination of MNP. As can be seen in Fig. 2, the MNP oxidized at about +760 mV on both bare CPE and Fe_3O_4@CPE surfaces. Although the capacitive current of Fe_3O_4 NPs modified CPE is higher than that of bare CPE, the peak current attributed to MNP oxidation at the modified electrode is found to be around three times higher than that obtained with bare CPE. In the literature, there are similar studies showing that both capacitive current and faradaic current of analyte increases as a result of the modification of CPE with Fe_3O_4 NPs [26–28]. Moreover, Fe_3O_4@CPE shows a better electrochemical signal than bare CPE due to obtaining a well-defined peak shape at the modified electrode. As a result, a remarkable enhancement was seen in the peak current of MNP at Fe_3O_4@CPE compared to the bare CPE. This enhancement can be attributed that Fe_3O_4NPs showing good electrocatalytic activity towards the oxidation of MNP. As reported literature that the loading of magnetite nanoparticles to bare electrode surfaces acts as a promoter by increasing the electro-active surface area [25,28]. Therefore, the efficient electrocatalytic effect of the modified electrode is attributed to increasing the electrocatalytic surface area and even providing an active surface for the adsorption of the analyte. Due to the good electrocatalytic efficiency of Fe_3O_4NPs, charge transfer between MNP and electrode surface is accelerated. As a result, the electrochemical

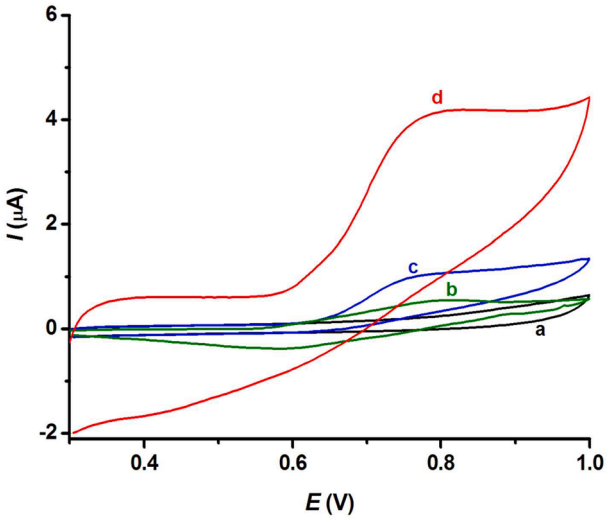

Fig. 2. CVs recorded at bare CPE (a, c) and Fe_3O_4@CPE (b, d) in the absence (a, b) and the presence of 0.10 mM MNP (c, d) in pH 2.0 BRBS containing 0.10 M KCl at 50 mV s^{-1}.

characteristics of MNP were significantly improved by the modification of Fe_3O_4 NPs.

3.5. Effect of pH on the response of MNP

The electrochemical response and determination of redox-active compounds are affected by the pH conditions of the electrolyte solution. Thus, to see the effect of pH on the response of MNP, CVs of 0.10 mM MNP at Fe_3O_4@CPE in BRBSs with varying pHs between 2.0 and 7.0 were recorded separately (Fig. 3A). It was observed that the oxidation peak potential of MNP shifted towards negative potentials with the increase of pH, and the peak currents related to the electrochemical responses were found to decrease gradually. A linear curve of oxidation peak potential of MNP (E) vs pH with the equation of $E(V) = -0.0491pH + 0.8345$ ($R^2 = 0.9983$) proves that H^+ directly takes part in the electrooxidation of MNP (Fig. 3B). It can be concluded that equal

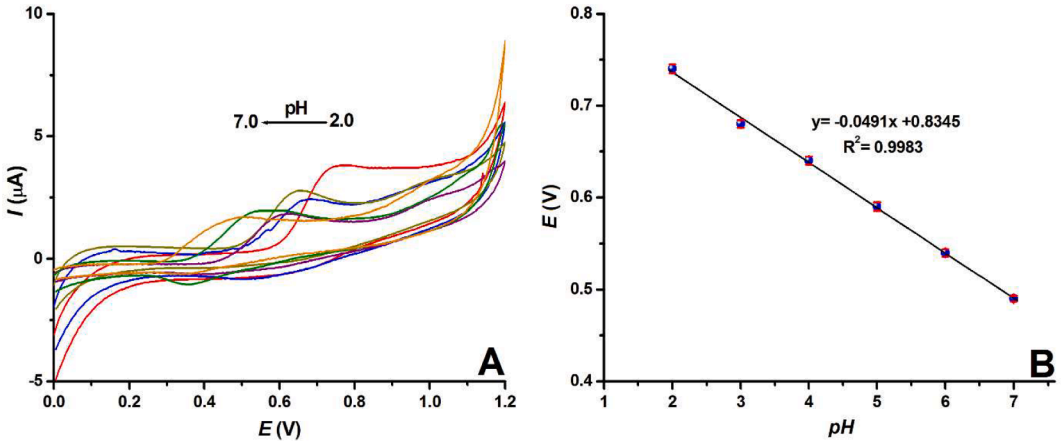

Fig. 3. **(A)** CVs of 0.10 mM MNP recorded at Fe_3O_4@CPE in BRBS containing 0.10 M KCl in the pH range from 2.0 to 7.0 and **(B)** the plot of oxidation peak potential (E) versus pH.

numbers of protons and electrons have participated in the irreversible oxidation of MNP at Fe_3O_4@CPE because the slope of this curve is nearly close the theoretical Nernstian slope value of 0.0592 V pH^{-1}. The BRBS with pH 2.0 where the electrochemical response of MNP oxidation is highest, was found to be the most suitable supporting electrolyte to be used. Obtaining high peak currents at acidic pH values can be explained by the protonation of MNP. At low pH values, MNP is protonated and the mass transport to the electrode surface increases resulting in the facilitation of its oxidation. The gradual decrease of the current as the pH increases from 2.0 to 7.0 is due to the decreasing protonated species and this supports the obtained result. Similar results were also obtained for the oxidation of some phenolic compounds at Fe_3O_4@CPE in the literature [23].

3.6. Effect of scan rate on the response of MNP

The effect of scan rate on the electrocatalytic oxidation peak current of MNP was examined by recording CVs of MNP at Fe_3O_4@CPE at various scan rates. Fig. S3A shows the CVs of 0.10 mM MNP in pH 2.0 BRBS containing 0.10 M KCl at increasing scan rates in the range from 10 to1200 mV s^{-1}. It can be seen in Fig. S3B, that the oxidation peak currents of MNP increased linearly with the increasing square root of scan rate with an equation of $I(\mu A) = 0.6798\nu^{1/2} + 0.1190$ (R^2 = 0.9973). This linear curve indicates that MNP is irreversibly oxidized at Fe_3O_4@CPE surface by a diffusion-controlled process. Linear curves of logarithmic oxidation peak current versus logarithm scan rate (Fig. S3C) support the diffusion-controlled process because the slope of 0.35 in this curve is close to the ideal slope of 0.5 reported for the diffusion-controlled process.

To calculate the electron number (n, for a totally irreversible reaction at 25 °C) that takes part in the electrocatalytic oxidation process of MNP, the following Eq. (2) [39] was used:

$$Ep - Ep/2 = \frac{47.7}{n\alpha} mV \quad (2)$$

E_p–$E_p/2$ was calculated as 50 mV for the oxidation peak of MNP which equals 0.95 of "nα". The electron transfer coefficient (α) is supposed to be 0.50 for a totally irreversible reaction [28]. The number of electrons (n) provided the value of 2. Thus, a mechanism given in Scheme 1 can be proposed for the electrocatalytic oxidation of MNP in Fe_3O_4@CPE. According to this mechanism, one H^+ and electron are separated from the –OH of the ammino hydroxyl group (–NH –OH) attached to the pyrimidine ring and a radical is formed on the oxygen. Also, the same process takes place in the –NH group of the amino hydroxyl group, forming a radical on the nitrogen atom. The electrocatalytic oxidation of MNP ends with a coupling of these radical electrons to form a nitroso group. The same electron number and similar oxidation mechanism were also proposed at rGO/GCE in the literature [38].

3.7. Evaluation of the analytical performance

The response of both bare CPE and Fe_3O_4@CPE towards the oxidation of MNP was investigated by differential pulse voltammetry and cyclic voltammetry. Before analytical performance studies, pH, pulse time, and pulse amplitude were optimized by recording differential pulse voltammograms (DPVs) of 250 μM MNP at Fe_3O_4@CPE. Fig. S4A shows DPVs of MNP at BRBS with varying pH between 2.0 and 8.0. As seen in the curve of peak current versus pH (Fig. S4B), the maximum peak was obtained from pH 2.0, these results agree with the CVs of MNP at various pH media. In addition, pulse time and pulse amplitude were optimized as 2 ms and 200 mV, respectively. Related voltammograms and curves are shown in Fig. S5 for pulse time and pulse amplitude. Although the maximum peak current was obtained at a pulse time of 1 ms, 2 ms was selected to obtain well-defined peaks.

DPVs of MNP based on its concentration in the range from 0 to 1500 μM for bare CPE and Fe_3O_4@CPE were given in Fig. S6A and Fig. 4A, respectively. Current versus concentration curves of dynamic and linear ranges are given in Fig. S6B-C and Fig. 4B-C for bare CPE and Fe_3O_4@CPE, respectively. As can be seen from these curves, the peak current of MNP was linearly changed dependent on its concentration in the range between 5.0 and 250 μM for bare CPE ($I(\mu A) = 0.045 \times [MNP](\mu M) - 0.161$, R^2 = 0.9994), while linearity range was found as 0.25–750 μM for Fe_3O_4@CPE ($I(\mu A) = 0.202 \times [MNP](\mu M) + 0.0862$, R^2 = 0.9993). The LOD was estimated to be 0.05 μM based on $3S_b/m$, where S_b is the standard deviation of the minimum MNP concentration that gives a measurable signal and m is the slope of the linear calibration curve. Fe_3O_4@CPE offered wide linear range for MNP determination compared with bare CPE and the modified electrode give 4.5 times more sensitive responses to MNP than CPE when the ratio of the slopes was taken into consideration. From DPV studies, the sensitivity of the modified electrode was calculated as 4591.0 μA mM^{-1} cm^{-2}. In addition, analytical performance studies were also performed by recording CVs of MNP, and linear ranges were found in the range from 2.5 to 750 μM for bare CPE ($I(\mu A) = 0.0048 \times [MNP](\mu M) - 0.0278$, R^2 = 0.9991) and 0.25–1500 μM for Fe_3O_4@CPE ($I(\mu A) = 0.0144 \times [MNP](\mu M) + 0.1778$, R^2 = 0.9994) were obtained (Fig. S7). It can be seen that although the calibration sensitivity of DPV is 14 times higher than that of CVs, CV has a wider linear range than that of DPV (in the range between 0.25 and 1500 μM).

In the literature, only one modified electrode has been reported for the voltammetric determination of MNP based on its oxidation at pH

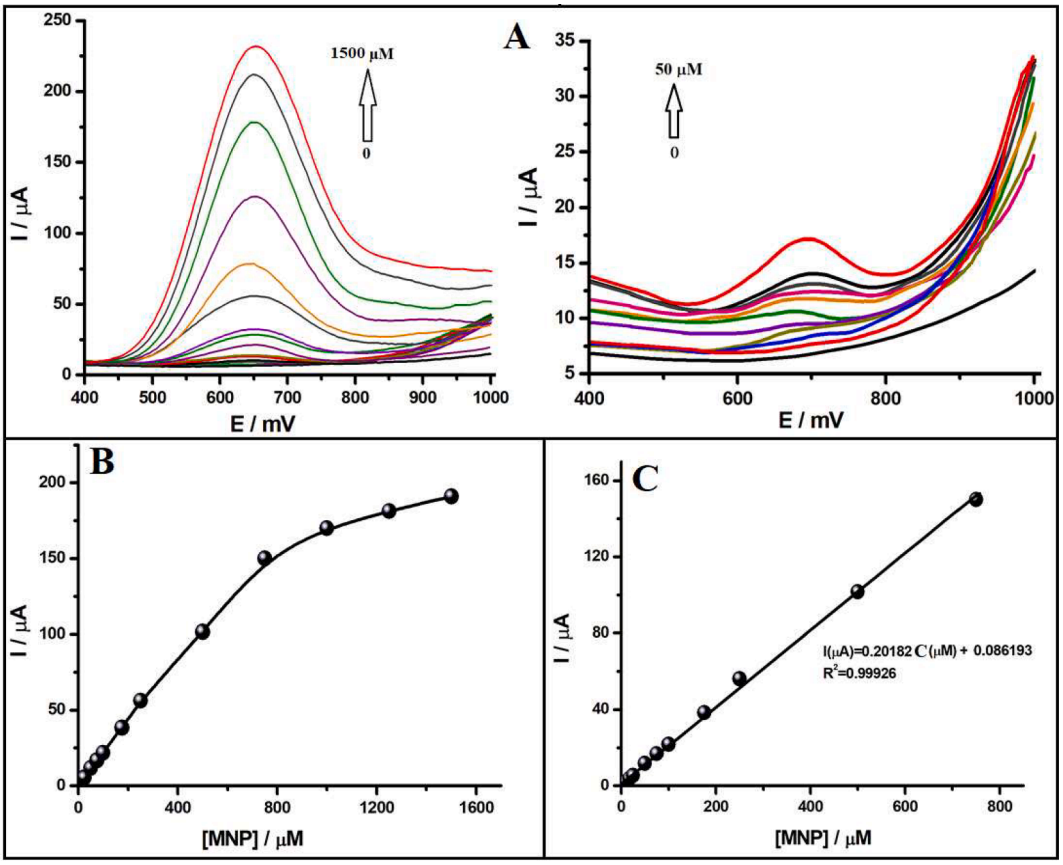

Fig. 4. DPVs of varying concentrations of MNP recorded at Fe_3O_4@CPE in pH 2.0 BRBS containing 0.10 M KCl at 20 mV s^{-1} (pulse time: 2 ms and pulse amplitude: 200 mV) (**A:** 0, 0.25, 0.5, 1, 2.5, 5, 7.5, 10, 17.5, 25, 50, 75, 100, 175, 250, 500, 750, 1000, 1250, 1500 µM MNP). Current versus concentration curves of dynamic **(C)** and linear **(D)** ranges.

9.0. A comparison of the analytical performance of the fabricated electrode with previously published rGO/GCE [38] was given in Table 1. This table shows that the Fe_3O_4@CPE has a much wider linear range than rGO/GCE and the sensitivity of the Fe_3O_4@CPE is competitive with rGO/GCE. Moreover, Fe_3O_4-modified CPE has some advantages such as a simple modification procedure, renewable surface, lower cost, and wider linear range over RGO/GCE [38]. The obtained results proved that Fe_3O_4@CPE provides a favorable platform for the determination of MNP. It can be concluded that these two electrodes exhibit the first electrochemical studies on the voltammetric determination of MNP.

3.8. Precision of the Fe_3O_4@CPE

The repeatability and reproducibility of the Fe_3O_4@CPE were also examined by recording DPVs of 250 µM MNP under previously optimized experimental conditions. To investigate the repeatability, 10 replicative intra-day measurements were performed in presence of MNP at Fe_3O_4@CPE. After each measurement, the surface of the electrode was washed with deionized water. The reproducibility of the modified electrode was tested at 10 newly prepared Fe_3O_4@CPE. The RSD values for repeatability and reproducibility were calculated as 3.79 % and 4.34 %, respectively. The obtained results (RSD $\leq$ 5.0 %) showed that Fe_3O_4@CPE exhibits high precisions for the determination of MNP.

Table 1
Comparison of the analytical performance of Fe_3O_4/CPE with previously reported rGO/GCE.

Electrode-Electrochemical method	Supporting electrolyte/ Oxidation potential of detected MNP.	LR (µM)	LOD (µM)	Sensitivity (µA mM^{-1} cm^{-2})
Fe_3O_4/CPE CV[1] and DPV[2] (This work)	pH 2.0 BRBS/750 mV vs Ag/AgCl (sat. KCl)	0.25 – 1500[1,2]	0.07[1] 0.05[2]	327.3[1] 4591.0[2]
rGO(GCE) SWV [38]	pH 9.0 BRBS/260 mV vs Ag/AgCl (sat. KCl)	0.09–4.57	0.03	–

3.9. Selectivity

To evaluate the selectivity, the voltammetric response of 100.0 µM MNP at Fe_3O_4@CPE was recorded in presence of various molecular and ionic species. Non-electroactive groups such as some cations, anions, and monosaccharides may interact with the analyte even though they do not give any signal or oxidation peak like MNP, for example, some metal ions may form a complex with MNP, or they can participate in electrostatic or intermolecular interaction with the analyte or analyte may be chemically oxidized by some molecules. In order to elucidate all these issues, it is useful to study of interference effect of some metal ions and anions on the analyte signal in interference studies, even if they are not electroactive. Therefore, the interference results of some non-electroactive ions or molecules, as well as electroactive compounds such as ascorbic acid (AA), dopamine (DA), and uric acid (UA) are summarized in Table 2. In addition, DPVs of the electroactive molecules (AA, DA, and UA) recorded at increasing concentrations alone and in the presence of the analyte (based on increasing interferant:analyte ratios using constant concentration as MNP:100 µM) are given in Fig. S8. Results were evaluated as the relative percent change (% Change in I_{pa} = $[(Ip_0–Ip_i)/Ip_0]x100$, Ip_0 = the oxidation current of MNP in the absence of interfering ions or molecules and Ip_i = oxidation current of MNP in

Table 2
The effects of interfering species on the DPV determination of MNP (n = 3).

Molecular Species	Fold	% Change in I_{pa}	Ionic Species	Fold	% Change in I_{pa}
Glucose	250	−7.4 ± 0.5	K^+	250	−6.3 ± 0.7
Sucrose	250	−8.3 ± 0.8	Na^+	250	−7.8 ± 0.9
Fructose	250	−3.8 ± 0.4	Mg^{2+}	250	−6.1 ± 0.8
Mannose	250	−7.8 ± 0.6	Zn^{2+}	250	−5.1 ± 0.7
Maltose	250	−4.5 ± 0.5	Ca^{2+}	250	−2.2 ± 0.4
H_2O_2	100	−7.7 ± 0.8	Cu^{2+}	5	+9.0 ± 1.1
Uric acid	0.1	+ 5.9 ± 1.2	Cl^-	250	−7.8 ± 0.9
Dopamine	1	+ 7.1 ± 1.8	NO_3^-	250	−5.2 ± 0.8
Ascorbic acid	5	+ 6.0 ± 1.5	SO_4^{2-}	250	−4.7 ± 0.7

the presence of interfering species in a known ratio of analyte to interference). It can be seen that UA, DA, and AA do not give any interference effect to 100 μM MNP in the interferant:analyte ratios of 0.1, 1, and 5, respectively. As seen from the figure, significant positive interferences above these ratios were observed for MNP, especially in UA. Considering the change in the current below 10 % as an evaluation criterion, it was concluded that common ions such as K^+, Na^+, Mg^{2+}, Zn^{2+}, Ca^{2+}, Cl^-, NO_3^-, SO_4^{2-} and some molecules such as H_2O_2, glucose, sucrose, fructose, mannose, and maltose did not show any interference effect on the oxidation of MNP even when each interfering compound concentration was 100 or 250 times higher than MNP. However, Cu^{2+} gave positive interference in the 5:1 of interferant:analyte ratios due to most probably formation of complex between Cu^{2+} and MNP. It can be concluded that the Fe_3O_4@CPE may offer high selectivity for voltammetric determination of MNP in samples containing these interfering species in the interferant:analyte ratios determined.

3.10. The application of Fe_3O_4@CPE on real samples

In the applicability of the electrochemical sensor, MNP with three different concentrations (25.0, 50.0, and 100.0 μM) was spiked into pharmaceutical tablet solutions including 50.0 μM MNP. Then, standard addition DPVs were recorded under optimized conditions. DPVs and standard addition calibration curves for un-spiked and spiked samples were given in Fig. S9. The experimental results and recovery values found between 98.2 and 100.6 % were summarized in Table 3. The MNP content was found to be 203 ± 6 mg/tablet, which is very close to the declared value of 200 mg MNP/tablet by a pharmaceutical company. The obtained results illustrated that the Fe_3O_4@CPE provides a highly accurate and precise determination of MNP in pharmaceutical samples.

4. Conclusion

According to our literature search, only one study on the electrochemical behavior and voltammetric determination of MNP is recently reported using rGO/GCE [38]. As a second study, the electrochemical study of MNP is described for the first time using highly efficient magnetite nanoparticles modified carbon paste electrode. The prepared Fe_3O_4@CPE shows high electrocatalytic activity towards irreversible oxidation of MNP compared with bare CPE. The fabricated electrode shows a quite wide linear range (between 0.25 and 750 μM) with a LOD of 0.05 μM from DPV results. In addition, Fe_3O_4@CPE was successfully used for the determination of MNP in real pharmaceutical samples and satisfactory results with high accuracy and precision have been obtained. It is considered to offer a good possibility as an alternative method for use in quality control units for the qualitative and quantitative analysis of MNP in samples. As a result, an accurate, sensitive, and reproducible electrochemical method has been developed and its applicability has been demonstrated using Fe_3O_4@CPE for the voltammetric determination of MNP.

Table 3
The results of applicability to pharmaceutical sample (n = 3).

Sample	Added standard MNP (μM)	Found MNP (μM)	Recovery (%)	Labeled amount (mg MNP/ tablet)	Found (mg MNP/ tablet)
Pharmaceutical Tablet	0	51.4 ± 1.6	–	200	203 ± 6
	25.0	76.8 ± 2.5	100.6	–	–
	50.0	101.5 ± 3.7	100.1	–	–
	100	148.7 ± 5.8	98.2	–	–

CRediT authorship contribution statement

Kader Vural: Software, Investigation, Validation. **Serkan Karakaya:** Software, Methodology, Writing – review & editing, Visualization. **Didem Giray Dilgin:** Investigation, Methodology. **Hatice İsmet Gökçel:** Writing – review & editing, Conceptualization. **Yusuf Dilgin:** Writing – review & editing, Conceptualization, Supervision.

Declaration of Competing Interest

The authors declare that they have no known competing financial interests or personal relationships that could have appeared to influence the work reported in this paper.

Data availability

Data will be made available on request.

Appendix A. Supplementary data

Supplementary data to this article can be found online at https://doi.org/10.1016/j.microc.2022.108195.

References

[1] WHO, WHO Director-General's opening remarks at the media briefing on COVID-19. https://www.who.int/director-general/speeches/detail/who-director-general-s-opening-remarks-at-the-media-briefing-on-covid-19—11-march-2020/, 11 Mach 2020 (accessed 20 June 2022).
[2] WHO, WHO Coronavirus (COVID-19) Dashboard, https://covid19.who.int/, 9 November 2022 (accessed 10 November 2022).
[3] F. Pourkarim, S. Pourtaghi-Anvarian, H. Rezaee, Molnupiravir: a new candidate for COVID-19 treatment, Pharmacol. Res. Perspect. 10 (2022) e00909.
[4] Molnupiravir and Drug Development at Emory https://news.emory.edu/tags/topic/molnupiravir/index.html (accessed 10 November 2022).
[5] E. Zarenezhad, M. Marzi, Review on molnupiravir as a promising oral drug for the treatment of COVID-19, Med. Chem. Res. 31 (2022) 232–243.
[6] R. Cross, Merck & Co. joins race for COVID-19 vaccines and therapies, Chem. Eng. News 98 (23) (2020).
[7] Development MaRBCtAaE-oNAC, https://www.businesswire. com/news/home/20200526005229/en/, 2003 (accessed 20 June 2022).
[8] Medicines and Healthcare products Regulatory Agency (MHRA), 2021. First oral antiviral for COVID-19, Lagevrio (molnupiravir), approved by MHRA" https://www.gov.uk/government/news/first-oral-antiviral-for-covid-19-lagevrio-molnupiravir-approved-by-mhra#:~:text=The%20antiviral%20Lagevrio%20(molnupiravir)%20is,Agency%20(MHRA)%20announced%20today/ 2021 (accessed 20 June 2022).
[9] U.S. Food and Drug Administration (FDA), Coronavirus (COVID-19) Update: FDA Authorizes Additional Oral Antiviral for Treatment of COVID-19 in Certain Adults. https://www.fda.gov/news-events/press-announcements/coronavirus-covid-19-update-fda-authorizes-additional-oral-antiviral-treatment-covid-19-certain#:~:text=Today%2C%20the%20U.S.%20Food%20and,progression%20to%20severe%20COVID%2D19%2C/, 2021 (accessed 20 June 2022).
[10] T. Reçber, S.S. Timur, S. Erdoğan Kablan, F. Yalçın, T.C. Karabulut, R.N. Gürsoy, H. Eroğlu, S. Kır, E. Nemutlu, A stability indicating RP-HPLC method for determination of the COVID-19 drug molnupiravir applied using nanoformulations in permeability studies, J. Pharm. Biomed. Anal. 214 (2022), 114693.
[11] Y.A. Sharaf, S. El Deeb, A.E. Ibrahim, A. Al-Harrasi, R.A. Sayed, Two green micellar HPLC and mathematically assisted UV spectroscopic methods for the simultaneous

determination of molnupiravir and favipiravir as a novel combined COVID-19 antiviral regimen, Molecules 27 (2022) 2330.
[12] A. Amara, S.D. Penchala, L. Else, C. Hale, R. FitzGerald, L. Walker, R. Lyons, T. Fletcher, S. Khoo, The development and validation of a novel LC-MS/MS method for the simultaneous quantification of molnupiravir and its metabolite ß-d-N4-hydroxycytidine in human plasma and saliva, J. Pharm. Biomed. Anal. 206 (2021), 114356.
[13] I.G. David, M. Buleandra, D.E. Popa, M.C. Cheregi, V. David, E.E. Iorgulescu, G. O. Tartareanu, Recent developments in voltammetric analysis of pharmaceuticals using disposable pencil graphite electrodes, Processes 10 (2022) 472.
[14] M. Güneş, S. Karakaya, T. Kocaağa, F. Yıldırım, Y. Dilgin, Sensitive voltammetric determination of oxymetazoline hydrochloride at a disposable electrode, Monatsh. Chem. 152 (2021) 1505–1513.
[15] M. Brycht, K. Konecka, K. Sipa, S. Skrzypek, V. Mirčeski, Electroanalysis of the anthelmintic drug bithionol at edge plane pyrolytic graphite electrode, Electroanalysis 31 (2019) 2246–2253.
[16] T. Erşan, D. Giray Dilgin, E. Kumrulu, U. Kumrulu, Y. Dilgin, Voltammetric determination of favipiravir used as an antiviral drug for the treatment of covid-19 at pencil graphite electrode, Electroanalysis (2022), https://doi.org/10.1002/elan.202200295 in press.
[17] E. Sohouli, M. Ghalkhani, M. Rostami, M. Rahimi-Nasrabadi, F. Ahmadi, A noble electrochemical sensor based on TiO_2@CuO-N-rGO and poly (L-cysteine) nanocomposite applicable for trace analysis of flunitrazepam, Mater. Sci. Eng., C 117 (2020), 111300.
[18] E. Sohouli, M. Ghalkhani, F. Shahdost-fard, E.M. Khosrowshahi, M. Rahimi-Nasrabadi, F. Ahmadi, Sensitive sensor based on TiO_2NPs nano-composite for the rapid analysis of Zolpidem, a psychoactive drug with cancer-causing potential, Mater. Today Commun. 26 (2021), 101945.
[19] S. Tajik, H. Beitollahi, S. Shahsavari, F.G. Nejad, Simultaneous and selective electrochemical sensing of methotrexate and folic acid in biological fluids and pharmaceutical samples using Fe_3O_4/ppy/Pd nanocomposite modified screen printed graphite electrode, Chemosphere 291 (3) (2022), 132736.
[20] N. Baig, M. Sajid, T.A. Saleh, Recent trends in nanomaterial-modified electrodes for electroanalytical applications, TrAC, Trends Anal. Chem. 111 (2019) 47–61.
[21] A. Waheed, M. Mansha, N. Ullah, Nanomaterials-based electrochemical detection of heavy metals in water: Current status, challenges and future direction, TrAC, Trends Anal. Chem. 105 (2018) 37–51.
[22] J.M. George, A. Antony, B. Mathew, Metal oxide nanoparticles in electrochemical sensing and biosensing: a review, Microchim. Acta 185 (2018) 358.
[23] P.C. Pwavodi, V.H. Ozyurt, S. Asir, M. Ozsoz, Electrochemical sensor for determination of various phenolic compounds in wine samples using Fe_3O_4 nanoparticles modified carbon paste electrode, Micromachines 12 (2021) 312.
[24] Z.O. Erdogan, S. Kucukkolbası, Fabrication of an electrochemical biosensor based on Fe_3O_4 nanoparticles and uricase modified carbon paste electrode for uric acid determination, Monatshefte für Chemie 152 (2021) 309–314.
[25] E. Al-Zahrani, M.T. Soomro, R.M. Bashami, A.U. Rehman, E. Danish, I.M.I. Ismail, M. Aslam, A. Hameed, Fabrication and performance of magnetite (Fe_3O_4) modified carbon paste electrode for the electrochemical detection of chlorite ions in aqueous medium, J. Environ. Chem. Eng. Part A 4 (4) (2016) 4330–4341.
[26] J.P. da Silveira, J.V. Piovesan, A. Spinelli, Carbon paste electrode modified with ferrimagnetic nanoparticles for voltammetric detection of the hormone estriol, Microchem. J. 133 (2017) 22–30.
[27] M.B. Gholivand, M. Torkashvand, E. Yavari, Electrooxidation behavior of warfarin in Fe_3O_4 nanoparticles modified carbon paste electrode and its determination in real samples, Mater. Sci. Eng., C 48 (2015) 235–242.
[28] M.P. Kingsley, P.B. Desai, A.K. Srivastava, Simultaneous electro-catalytic oxidative determination of ascorbic acid and folic acid using Fe_3O_4 nanoparticles modified carbon paste electrode, J. Electroanal. Chem. 741 (2015) 71–79.
[29] W. Zhang, J. Zheng, J. Shi, Z. Lin, Q. Huang, H. Zhang, C. Wei, J. Chen, S. Hu, A. Hao, Nafion covered core–shell structured Fe_3O_4@graphene nanospheres modified electrode for highly selective detection of dopamine, Anal. Chim. Acta 853 (2015) 285–290.
[30] X. Li, X. Huang, D. Liu, X. Wang, S. Song, L. Zhou, H. Zhang, Synthesis of 3D hierarchical Fe_3O_4/graphene composites with high lithium storage capacity and for controlled drug delivery, J. Phys. Chem. C 115 (44) (2011) 21567–21573.
[31] J.-K. Xu, F.-F. Zhang, J.-J. Sun, J. Sheng, F. Wang, M. Sun, Bio and nanomaterials based on Fe_3O_4, Molecules 19 (2014) 21506–21528.
[32] H.S. El-Desoky, A.M. Beltagi, M.M. Ghoneim, A.I. El-Hadad, The first utilization of graphene nano-sheets and synthesized Fe_3O_4 nanoparticles as a synergistic electrodeposition platform for simultaneous voltammetric determination of some toxic heavy metal ions in various real environmental water samples, Microchem. J. 175 (2022), 106966.
[33] H. Yin, Y. Zhou, Q. Ma, S. Ai, Q. Chen, L. Zhu, Electrocatalytic oxidation behavior of guanosine at graphene, chitosan and Fe_3O_4 nanoparticles modified glassy carbon electrode and its determination, Talanta 82 (4) (2010) 1193–1199.
[34] Y. Cheng, Y. Liu, J. Huang, K. Li, Y. Xian, W. Zhang, L. Jin, Amperometric tyrosinase biosensor based on Fe_3O_4 nanoparticles-coated carbon nanotubes nanocomposite for rapid detection of coliforms, Electrochim. Acta 54 (9) (2009) 2588–2594.
[35] D. Cao, N. Hu, Direct electron transfer between hemoglobin and pyrolytic graphite electrodes enhanced by Fe_3O_4 nanoparticles in their layer-by-layer self-assembly films, Biophys. Chem. 121 (3) (2006) 209–217.
[36] H. Teymourian, A. Salimi, S. Khezrian, Fe_3O_4 magnetic nanoparticles/reduced graphene oxide nanosheets as a novel electrochemical and bioeletrochemical sensing platform, Biosens. Bioelectron. 49 (2013) 1–8.
[37] V. Riahifar, N. Haghnazari, F. Keshavarzi, E. Ahmadi, A sensitive voltammetric sensor for methamphetamine determination based on modified glassy carbon electrode using Fe_3O_4@poly pyrrole core-shell and graphene oxide, Microchemical Journal 170 (2021), 106748.
[38] S.E. Kablan, T. Reçber, G. Tezel, S.S. Timur, C. Karabulut, T.C. Karabulut, H. Eroğlu, S. Kır, E. Nemutlu, Voltammetric sensor for COVID-19 drug Molnupiravir on modified glassy carbon electrode with electrochemically reduced graphene oxide, J. Electroanal. Chem. 920 (2022), 116579.
[39] V.V. Tkach, M.V. Kushnir, S.C. de Oliveira, I.M. Shevchenko, V.M. Odyntsova, V. M. Omelyanchik, L.O. Omelyanchik, O.V. Luganska, V.V. Kopiika, Z.O. Kormosh, Y.G. Ivanushko, V.V. Kryvetskyi, I.I. Kryvetska, I.V. Kryvetskyi, N. R. Yemelianenko, V.F. Rusnak, P. Yagodynets, Z.Z. Masna, L.V. dos Reis, Theoretical description for anti-COVID-19 drug molnupiravir electrochemical determination over the poly-((1,2,4-triazole)-co-(squaraine dye)) composite with cobalt (III) oxyhydroxide, Biointerface Res. Appl. Chem. 13 (1) (2023) 74.
[40] K. Zhang, W. Yang, Y. Liu, K. Zhang, Y. Chen, X. Yin, Laccase immobilized on chitosan-coated Fe_3O_4 nanoparticles as reusable biocatalyst for degradation of chlorophenol, J. Mol. Struct. 1220 (2020), 128769.
[41] G. Emir, S. Karakaya, S. Ayaz, D. Giray Dilgin, Y. Dilgin, Electrocatalytic oxidation and flow injection analysis of formaldehyde at binary metal oxides (Co_3O_4–NiO and CuO–Co_3O_4) modified pencil graphite electrodes, Monatsh. Chem. 152 (2021) 1491–1503.